

Supporting Information

The Anti-Biofouling Properties of Superhydrophobic Surfaces are Short-Lived

Gi Byoung Hwang ^a, Kristopher Page ^a, Adnan Patir ^a, Sean P. Nair ^b, Elaine Allan ^b, and Ivan P. Parkin ^{a*}

^aMaterials Chemistry Research Centre, Department of Chemistry, University College London, 20 Gordon Street, London, WC1H 0AJ, United Kingdom

^bDivision of Microbial Diseases, UCL Eastman Dental Institute, University College London, 256 Gray's Inn Road, London WC1X 8LD, United Kingdom

* To whom correspondence should be addressed.

E-mail: i.p.parkin@ucl.ac.uk Tel: 44(0)207 679 4669

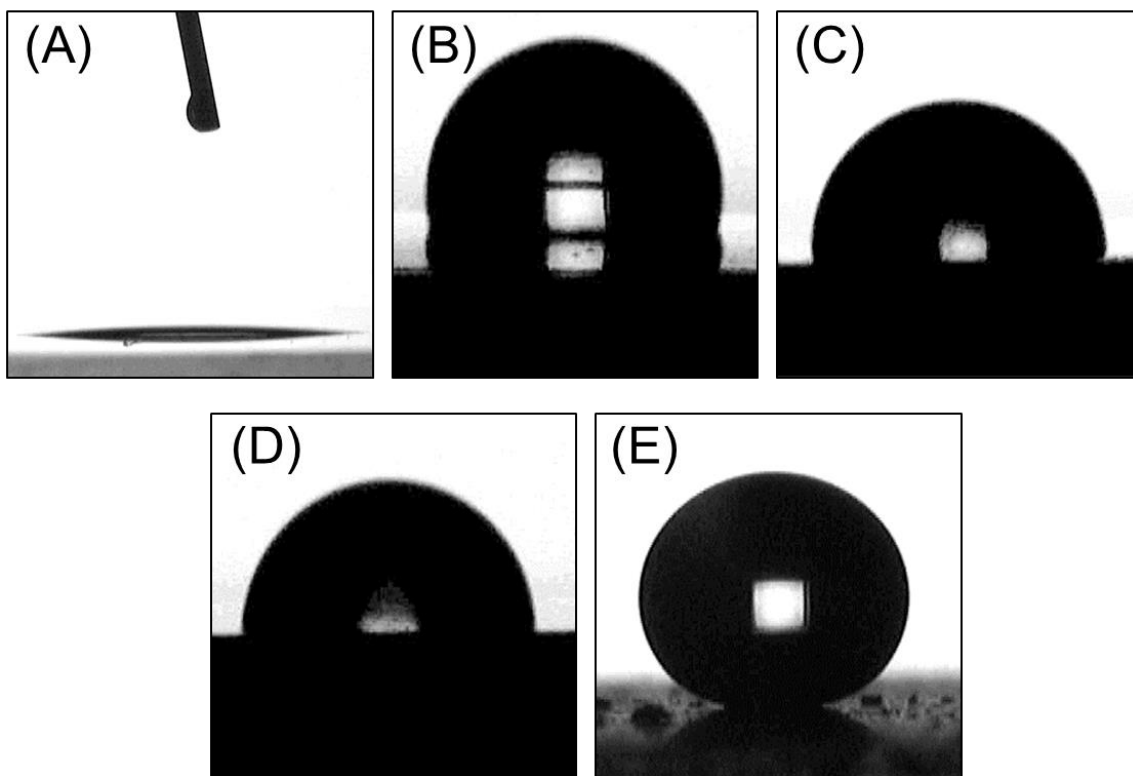


Figure S1. Water contact angle of (a) glass slide (b) polyurethane (PU) (c) white polystyrene sheet A (WPSA), (d) white polystyrene sheet B (WPSB), and (e) superhydrophobic surface (SHS)

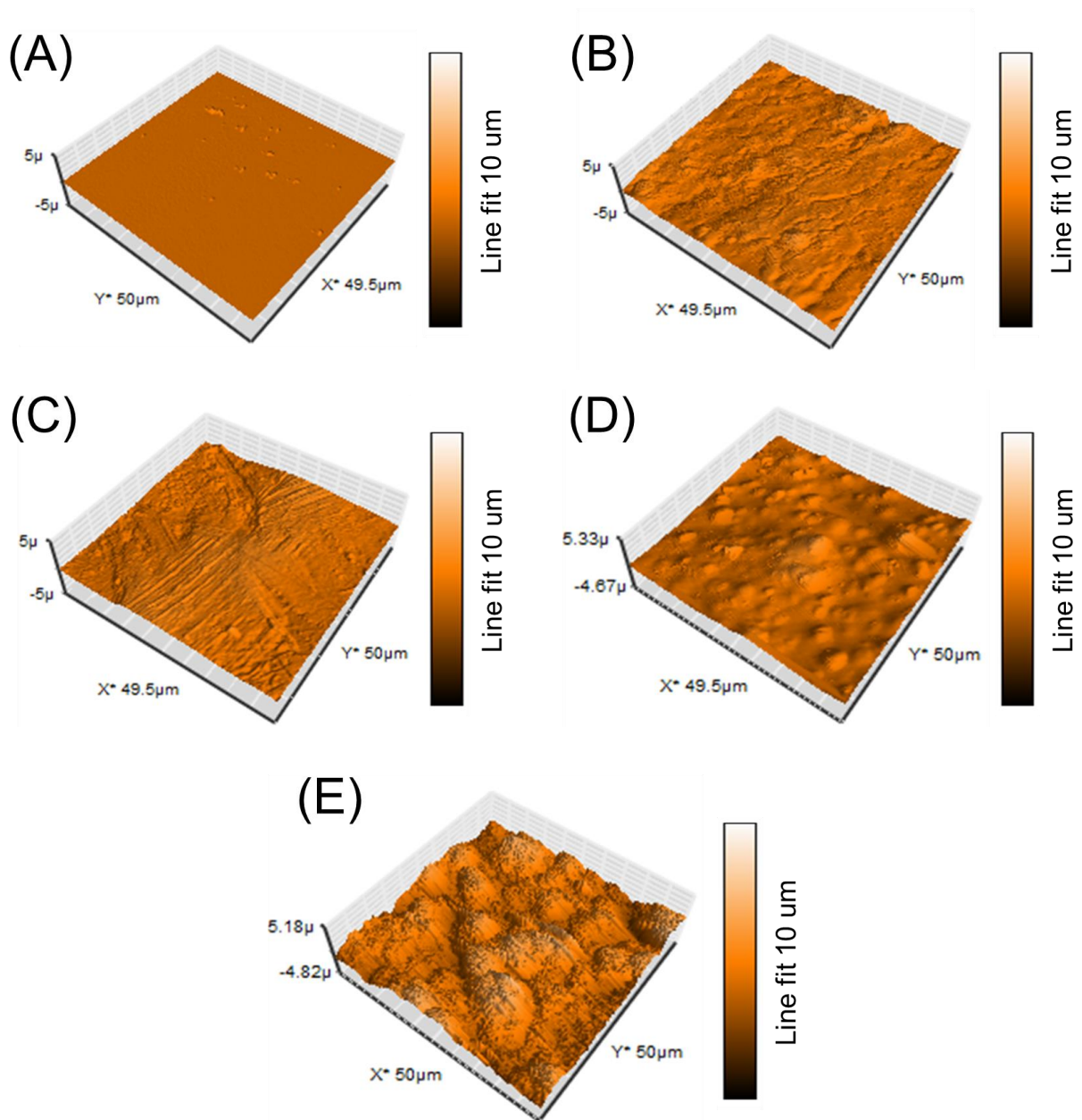


Figure S2. Topography images of (a) glass slide (b) polyurethane (PU) (c) white polystyrene sheet A (WPSA), (d) white polystyrene sheet B (WPSB), and (e) superhydrophobic surface (SHS)

Figure S3 shows the water contact angle of *S. aureus*, MRSA, *E. coli*, and CRE biofilms. The bacteria were plated on agar (mannitol salt agar for *S. aureus* and MRSA, and MacConkey agar for *E. coli* and CRE) and after 24 h incubation at 37°C, the water contact angle on the bacterial film was measured using a contact angle meter. The bacterial films all gave a water contact angle of <math><15^\circ</math>, indicating hydrophilicity.

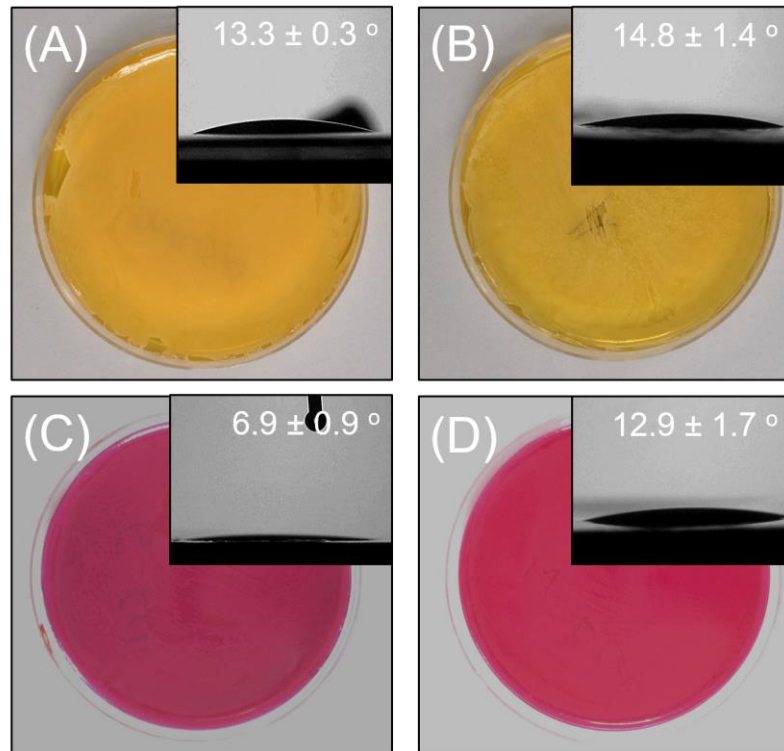


Figure S3. Water contact angle on (a) *S. aureus*, (b) MRSA, (c) *E. coli*, and (d) CRE colonies grown on agar.

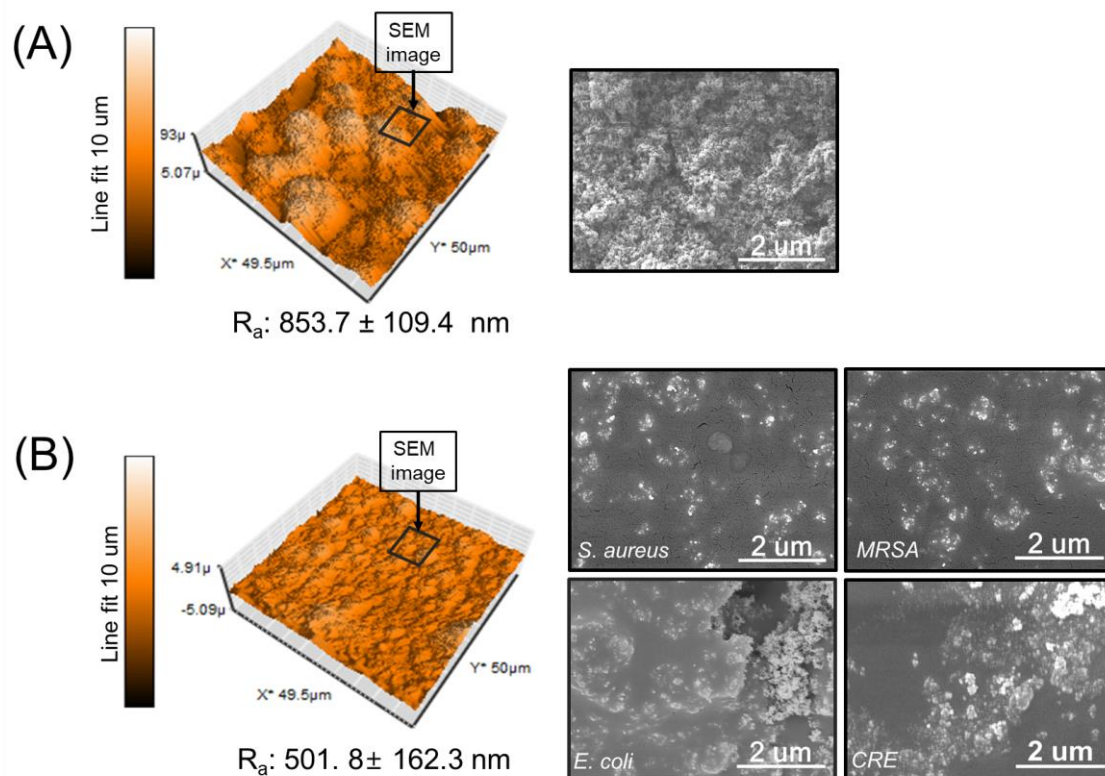


Figure S4. AFM Topography and a SEM image of the superhydrophobic surface (a) before and (b) after 24 h bacterial exposure in BHI and PBS

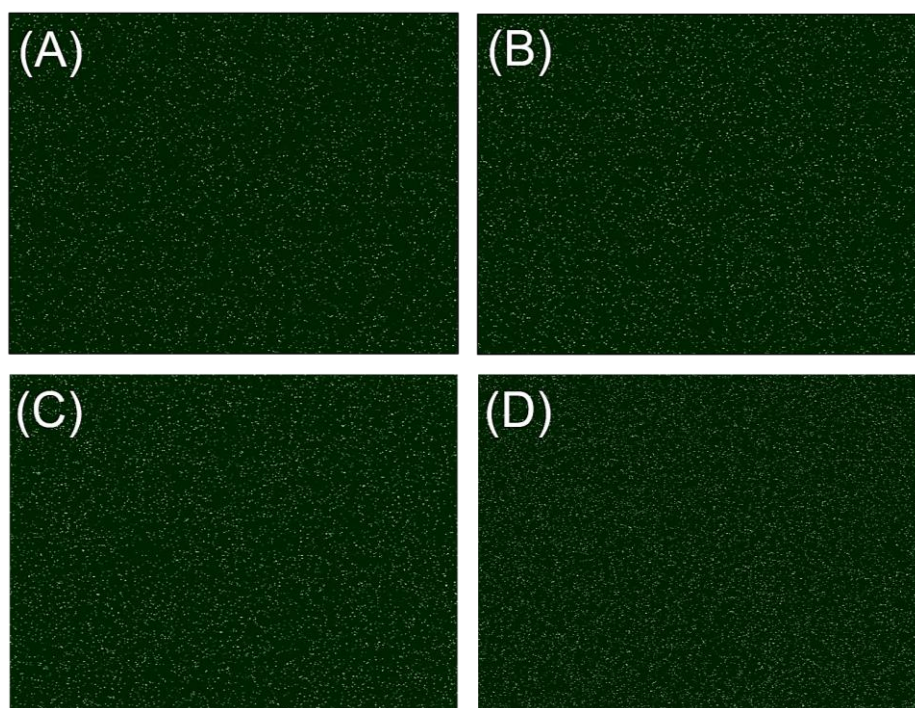


Figure S5. Confocal images of (a) *S. aureus*, (b) MRSA, (c) *E. coli*, and (d) CRE attached on the superhydrophobic surface.

Fabrication of superhydrophobic surface A (SHSA)

NeverWet spray contains step one spray for producing rough surface and step two spray for causing a reduction of surface energy. At the first stage, a glass slide was coated with step one spray twice, and then it was allowed to dry for 30 min. In the second step the sample was coated by the step two spray and then dried for 30 min.

Fabrication of superhydrophobic surface B (SHSB)

2 g of PDMS (Dow Corning SYLGARD184, with 10% curing agent) and 2.75 g of SiO₂ nanoparticles (5-15 nm in size, Sigma-Aldrich, St. Louis, MO, USA) were mixed in 20 mL of hexane (Sigma-Aldrich, St. Louis, MO, USA) under sonication. The glass slide was dipped into the solution for 5 s. Then, the glass was slowly withdrawn, retaining a thin solution film on its surface. After the solvent was mostly evaporated, the coating layer was cured at 100 °C for 2 h and then allowed to cool to room temperature.

SHSA was fabricated using NeverWet spray (Neverwet, LLC, USA) and SHSB was produced using PDMS, SiO₂ nanoparticles, and hexane. As shown in Table S1 and Figure S6, SHSA and B showed a water contact angle of >150 °, low rolling off angle (<2.8 °) and contact angle hysteresis (<2.3 °). AFM analysis showed that the surface roughness values of SHSA and B were 1015 and 805.2 nm, respectively. Bacterial adhesion on SHSA and SHSB was tested for MRSA for 24 h in BHI and PBS. As shown in Figure S7, it was observed that the number of bacteria attached on both SHSs was higher than the glass slide, PU, WPSA and WPSB. A statistically significant correlation between the number of attached bacteria and the surface roughness of the samples was confirmed; $0.095 < r < 0.96$ (Pearson correlation coefficient (PCC)) between other samples and SHSA in PBS and BHI; $0.96 < r < 0.99$ (PCC) between other samples and SHSB in PBS and BHI. The relationship of the water contact angle (PCC: $0.082 < r < 0.91$) was lower than that of surface roughness.

Table S1 Water contact angle, rolling off angle, contact angle hysteresis, and surface roughness of superhydrophobic surface A and B.

	Superhydrophobic surface A	Superhydrophobic surface B
Water contact Angle (°)	152.4 ± 1.8	153.4 ± 2.0
Rolling off angle (°)	0 ± 0	2.8 ± 1.3
Contac angle Hysteresis (°)	2.3 ± 1.2	1.5 ± 1.1
Surface Roughness (R_a , nm)	1015.0 ± 113.3	805.2 ± 227

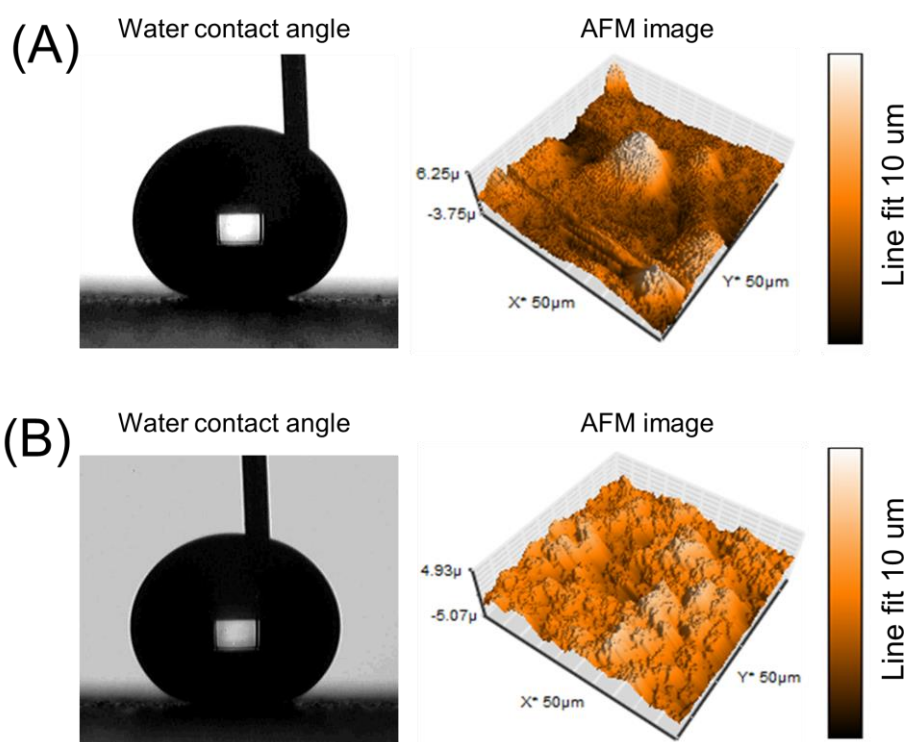


Figure S6. Image of water contact angle and topography of (a) superhydrophobic surface A and (b) B

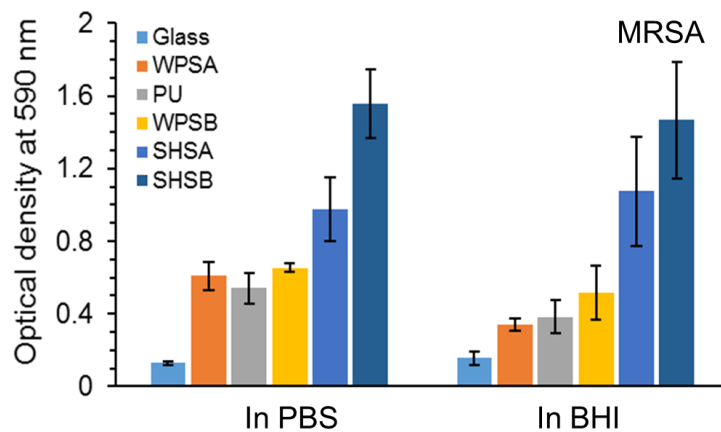


Figure S7. Comparison of MRSA attachment on glass slide, polyurethane (PU), white polystyrene sheet A (WPSA), white polystyrene sheet B (WPSB), and superhydrophobic surface A (SHSA) and B (SHSA) after 24 h bacterial exposure

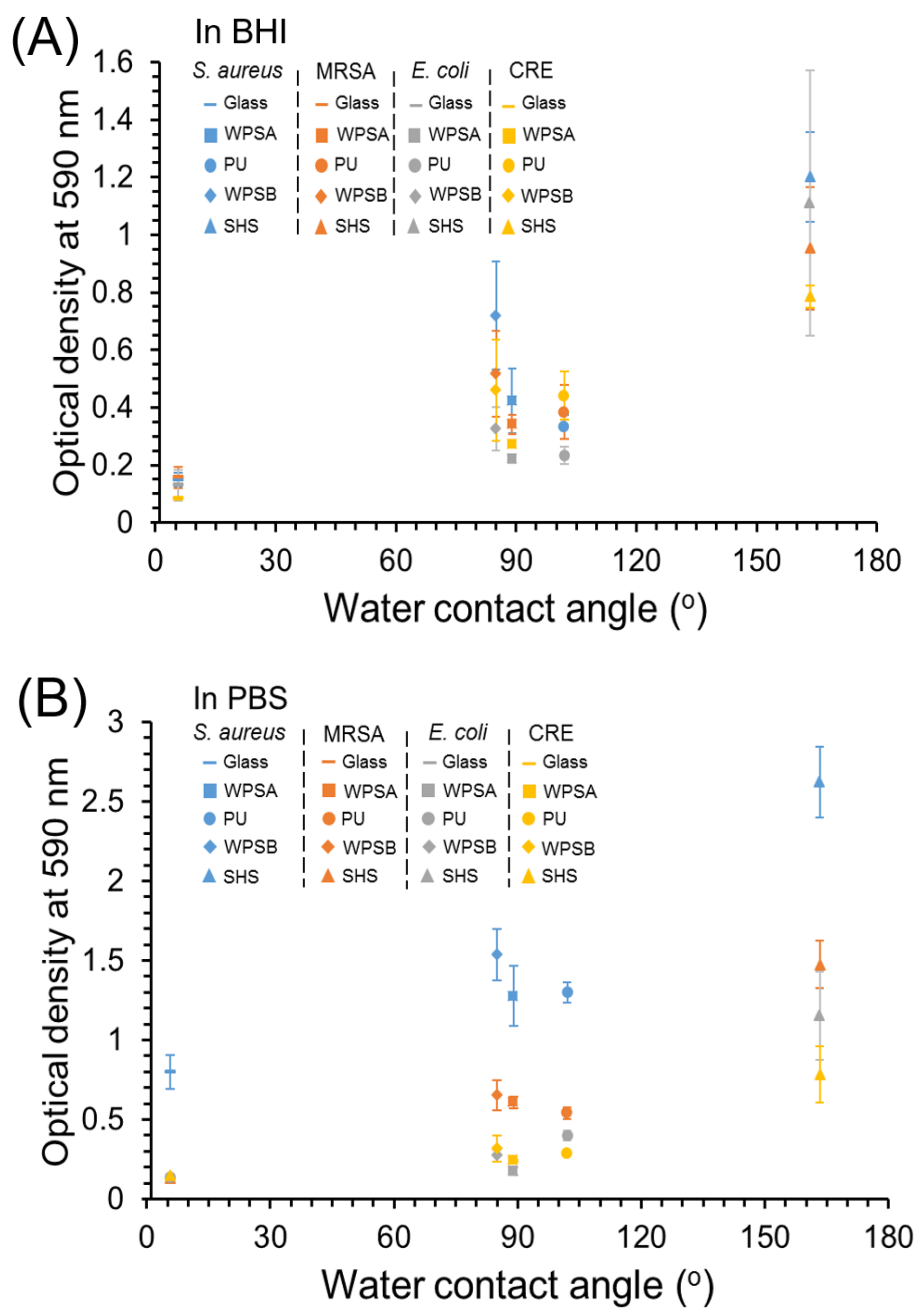
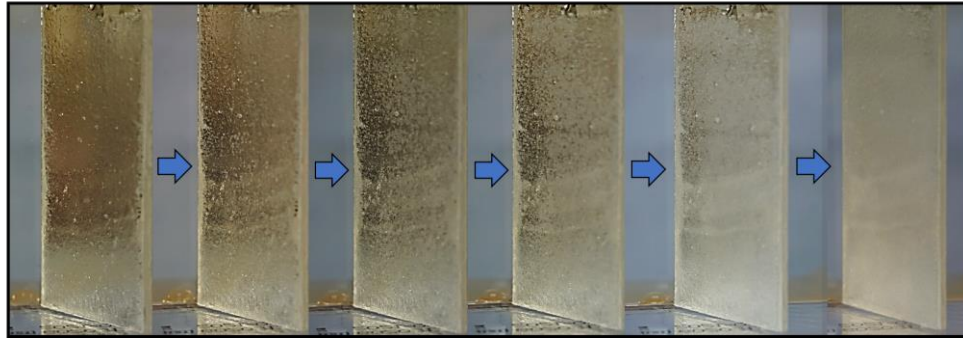
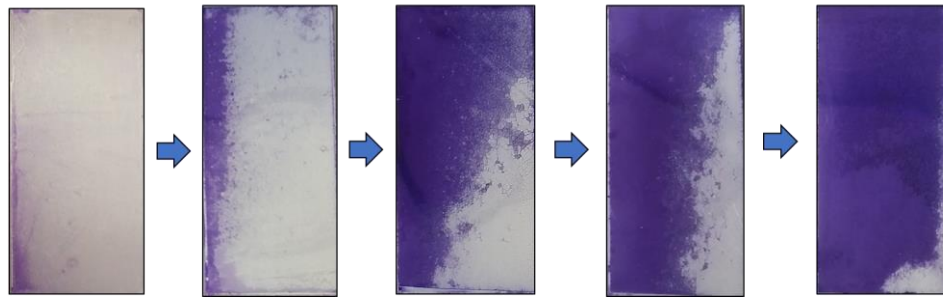


Figure S8. Correlation between the quantity of attached bacteria and the water contact angle of the materials: (a) in BHI broth and (b) in PBS.

(A) Disappearance process of plastron effect (air-bubbles) across superhydrophobic surface



(B) Process of bacteria surface (*S. aureus*) colonization across superhydrophobic surface



(C) Process of WCA reduction across superhydrophobic surface by CRE

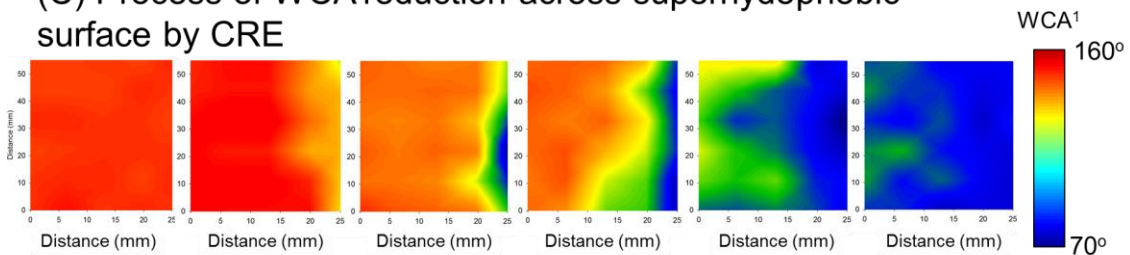


Figure S9. Pattern comparison of (a) plastron disappearance, (b) bacteria colonization, and (c) WCA reduction across superhydrophobic surface.

¹WCA: Water contact angle

As shown Figure S9, bacterial colonization and the reduction of water contact angle across the superhydrophobic surface mirrored the pattern of air-bubble disappearance on the surface. The phenomenon started from the edge and progressed across the surface. This indicates that bacterial colonization correlates with the pattern of air-bubble disappearance on the superhydrophobic surface (Figure S10) although it is slower than the pace of the bubble disappearance. The delayed colonization can be explained in that, as shown in Figure S10, the superhydrophobic surface has a fine polymer brush resulted from PFOTES, self-assembled monolayer, bonding to the TiO₂ surface,¹⁻² and it produces very weak adhesion force on the

adhering bacteria resulting in low interaction between bacteria and the surface indicating slow formation of polymer bridge between them.³⁻⁹ As a result, bacterial surface colonization was slow.

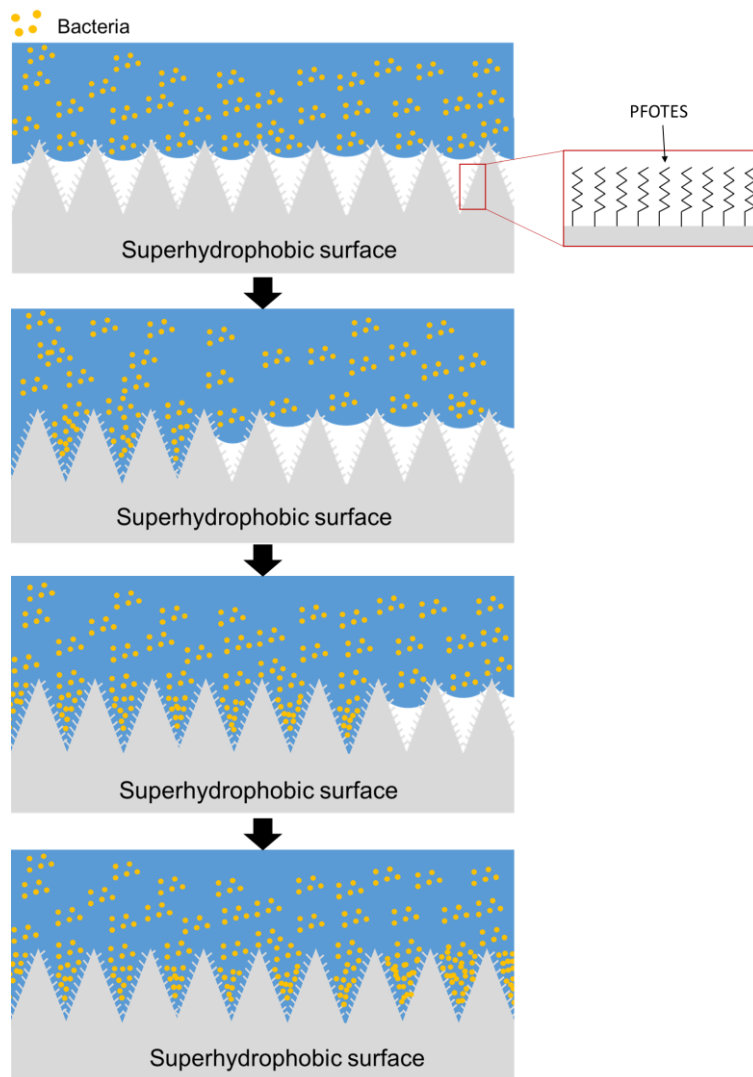
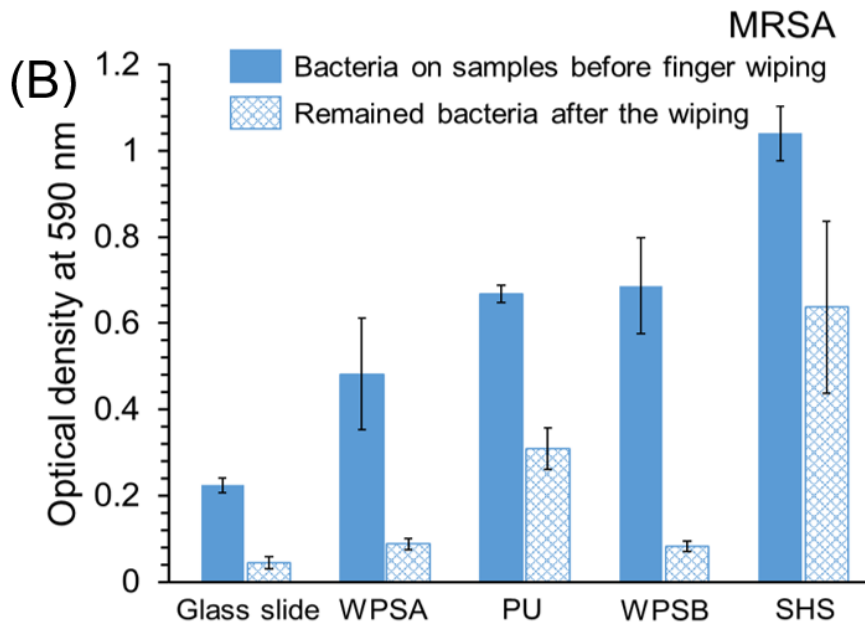
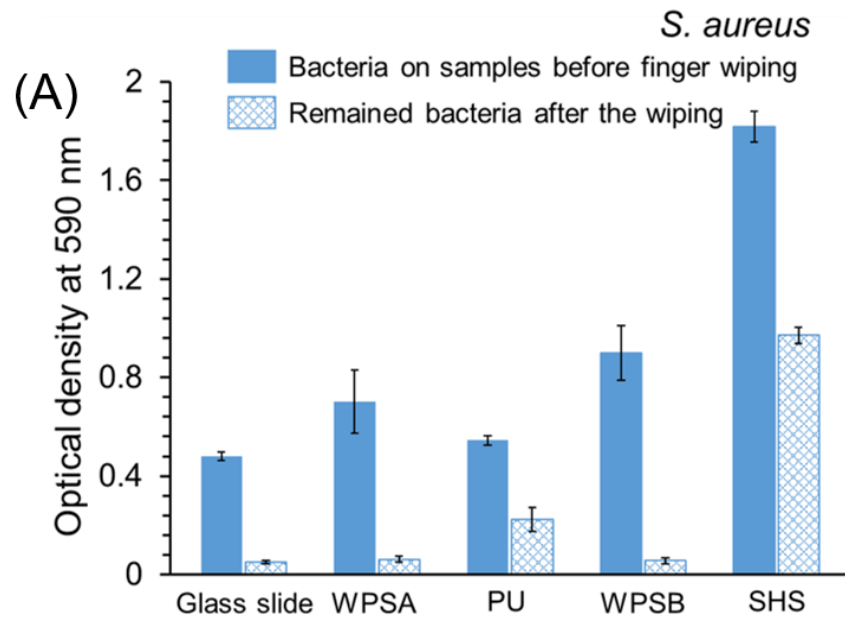


Figure S10. Relationship of bacterial adhesion and air-bubble disappearance across a superhydrophobic surface



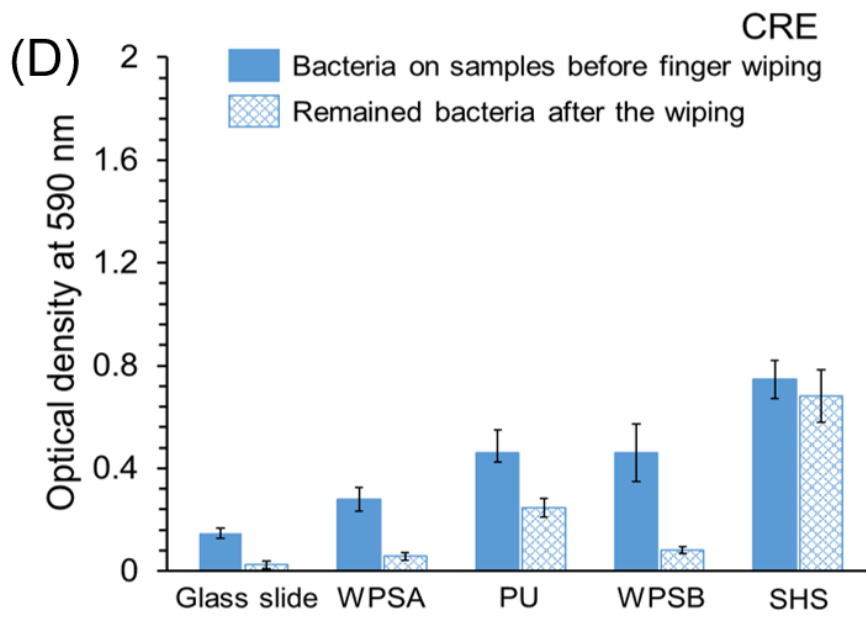
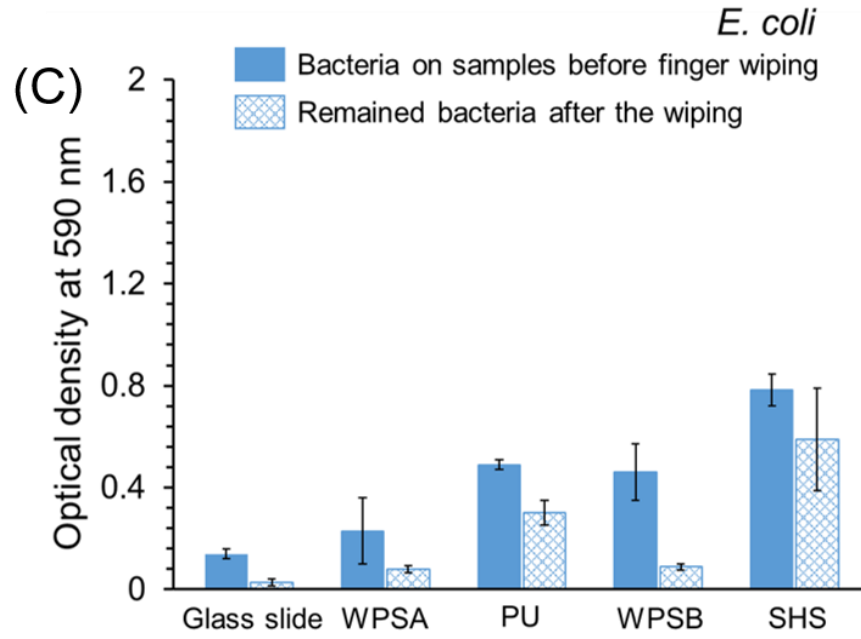


Figure S11. Comparison of the quantity of bacteria on the materials before and after finger wiping: (a) *S. aureus*, (b) MRSA, (c) *E. coli*, and (d) CRE.

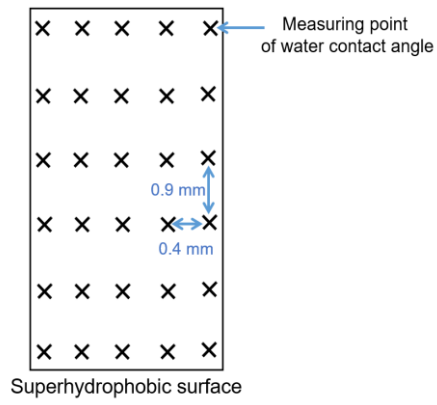


Figure S12. Measurement of water contact angle cross superhydrophobic surface

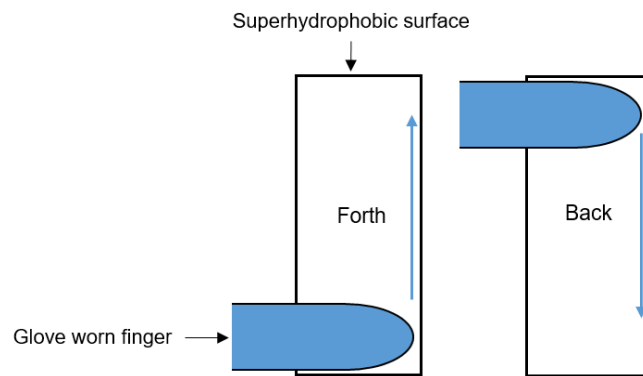


Figure S13. Finger wiping test

Video Legends

Video S1. Water repellent test on superhydrophobic surface

REFERENCES

- (1) Cech, J.; Taboryski, R. Stability of FDTS Monolayer Coating on Aluminum Injection Molding Tools. *Appl. Surf. Sci.* **2012**, *259*, 538–541
- (2) Barlow, S. M.; Raval, R. Complex Organic Molecules at Metal Surfaces: Bonding, Organisation and Chirality. *Surf. Sci. Rep.* **2003**, *50*, 201-341.
- (3) Muszanska, A. K.; Nejadnik, M. R.; Chen, Y.; van den Heuvel, E. R.; Busscher, H. J.; van der Mei, H. C.; Norde, W. Bacterial Adhesion Forces with Substratum Surfaces and the Susceptibility of Biofilms to Antibiotics. *Antimicrob. Agents Chemother.* **2012**, *56*, 4961-4964.
- (4) Harapanahalli, A. K.; Chen, Y.; Li, J.; Busscher, H. J.; van der Mei, H. C. Influence of Adhesion Force on *icaA* and *cidA* Gene Expression and Production of Matrix Components in *Staphylococcus aureus* Biofilms. *Appl. Environ. Microbiol.* **2015**, *81*, 3369-3378.
- (5) Emerson, R. J. t.; Bergstrom, T. S.; Liu, Y.; Soto, E. R.; Brown, C. A.; McGimpsey, W. G.; Camesano, T. A. Microscale Correlation Between Surface Chemistry, Texture, and the Adhesive Strength of *Staphylococcus epidermidis*. *Langmuir* **2006**, *22*, 11311-11221.
- (6) Liu, Y.; Strauss, J.; Camesano, T. A. Adhesion Forces Between *Staphylococcus epidermidis* and Surfaces Bearing Self-Assembled Monolayers in the Presence of Model Proteins. *Biomaterials* **2008**, *29*, 4374-4382.
- (7) Alam, F.; Balani, K. Adhesion Force of *Staphylococcus aureus* on Various Biomaterial Surfaces. *J. Mech. Behav. Biomed. Mater.* **2017**, *65*, 872-880.
- (8) Nejadnik, M. R.; van der Mei, H. C.; Norde, W.; Busscher, H. J. Bacterial Adhesion and Growth on a Polymer Brush-Coating. *Biomaterials* **2008**, *29*, 4117-4121.
- (9) Garrett, T. R.; Bhakoo, M.; Zhang, Z. Bacterial Adhesion and Biofilms on Surfaces. *Prog. Nat. Sci.* **2008**, *18*, 1049-1056.